The 1996 equatorial Atlantic warm event: Origin and mechanisms

S. Illig,[1] D. Gushchina,[2] B. Dewitte,[1] N. Ayoub,[1] and Y. du Penhoat[1]

[1] We investigate the interannual warm event that occurred in the equatorial Atlantic in boreal spring-summer 1996. The role of local coupled air-sea interactions versus Tropical Pacific remote forcing is analysed using observations and ensemble experiments of an intermediate coupled model of the Tropical Atlantic. Results show that the persistent anomalous cold conditions in the Tropical Pacific over 1995–96 were favorable to the growth of the local air-sea interactions that led to the 1996 warming in the equatorial Atlantic. Based on the estimation of the changes in the Walker circulation over the Pacific and Atlantic for the meteorological reanalyses and the coupled model, a mechanism of Pacific-Atlantic equatorial connection is proposed to explain this particular warm episode. **Citation:** Illig, S., D. Gushchina, B. Dewitte, N. Ayoub, and Y. du Penhoat (2006), The 1996 equatorial Atlantic warm event: Origin and mechanisms, *Geophys. Res. Lett.*, *33*, L09701, doi:10.1029/2005GL025632.

1. Introduction

[2] The Equatorial Atlantic (EA) interannual variability can be explained by local air-sea interactions, maintained and/or triggered by either external stochastic forcing [*Zebiak*, 1993] or coherent remote forcing mostly originating from the Tropical Pacific (TP) [*Delecluse et al.*, 1994; *Illig and Dewitte*, 2006]. An atmospheric equatorial teleconnection that operates through changes in the Walker circulation cells in both basins plays a fundamental role [*Wang*, 2002]. How those changes in the zonal equatorial atmospheric circulation take place may provide insights on how interannual events develop in the EA.

[3] In boreal spring-summer 1996, while the eastern TP was under cold/neutral conditions, the EA ocean went through anomalous warm conditions (Figure 1). *Handoh and Bigg* [2000] (hereinafter referred to as HB00) suggest that this warm event, followed by cold conditions in 1997, was the signature of the Atlantic equatorial mode [*Zebiak*, 1993; *Latif and Grötzner*, 2000; *Wang*, 2002], initiated by intense Wind Stress Anomalies (WSA) in the western EA in fall 1995. These would have been caused by local atmospheric variability in the Tropical American convection center, possibly remotely forced by the TP variability. Here, in light of HB00's results, we further investigate the respective role of local air-sea interactions and TP remote forcing during this particular warm event by analyzing observations, meteorological reanalyses and ensemble simulations of an intermediate coupled model of the EA.

[1]Laboratoire d'Etudes en Géophysique et Océanographie Spatiales, Toulouse, France.
[2]Geographical Faculty, Moscow State University, Moscow, Russia.

Focusing on the atmospheric teleconnection pattern in 1995–96, a triggering mechanism of the EA 1996 warming is then proposed.

2. Data and Model

[4] Our analysis is based on weekly averaged data of the Reynolds Sea Surface Temperature (SST) [*Reynolds and Smith*, 1994], and T/P and ERS1/2 altimetric Sea Level (SL) [*Le Traon et al.*, 1998]. The daily NCEP/NCAR reanalysis fields [*Kalnay et al.*, 1996] are used as an estimation of the atmospheric anomalous conditions.

[5] Our Tropical Intermediate coupled Model for Atlantic Climate Studies (TIMACS) is designed such that air-sea coupling is explicitly taken into account in the EA, while observed SST forcing is prescribed elsewhere. The oceanic component consists of the EA 6 baroclinic mode Ocean Linear Model (OLM) developed by *Illig et al.* [2004], in which a mixed layer model similar to *Zebiak* [1993] is embedded. The atmospheric component is the global Quasi-equilibrium Tropical Circulation Model (QTCM) from *Neelin and Zeng* [2000]. An extensive description of TIMACS components, spin-up and coupling procedures is given by *Illig and Dewitte* [2006], where TIMACS is extensively validated from observations and forced OGCM simulations over 1982–2001 for monthly-averaged outputs. Here we focus on a shorter period of time and perform analysis on daily-averaged outputs.

[6] Observed and simulated interannual anomalies are estimated with respect to daily climatologies computed over the 1993–96 period. This period encompasses all the data covering period and excludes the big 1997/98 ENSO event, which signature could bias our estimation of the interannual anomalies. For a better representation, a 15-day running mean is applied along the equatorial sections.

3. The EA 1996 Warm Event

[7] Throughout the boreal spring and summer 1996, the EA went through anomalous conditions [HB00]. In the Gulf of Guinea, oceanic warm conditions took place from early 1996 to early autumn 1996 (Figures 1b and 2a): In the eastern EA, a deeper thermocline and a weakened equatorial upwelling led to a less pronounced cold tongue and larger than normal SL (Figure 1a). This interpretation of observed variability is supported by the results of the OLM simulations (see below). In June 1996, anomalies exceeded 1.25°C in SST and 4 cm in SL in ATL3 (20°W–0°E; 3°S–N), with spatial structures similar to the coupled equatorial mode described by *Zebiak* [1993] (Figure 1d).

[8] This ocean warming imprints the EA troposphere as evidenced from the NCEP wind velocity field (Figures 1b and 1c): In the low (upper) troposphere, the westerly (easterly) wind anomalies developed along the equator in
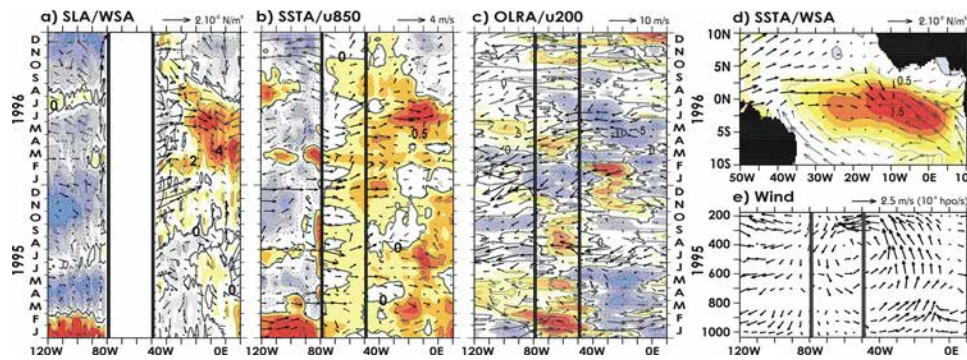
Figure 1. (a) Hovmuller of T/P+ERS SLA. Contour interval (CI) is 2 cm. Arrows: NCEP WSA. (b) Hovmuller of Reynolds SSTA. CI is 0.5°C. Arrows: NCEP 850 mb wind anomalies. (c) Hovmuller of the NCEP OLRA. CI is 5 W/m². Arrows: NCEP 200 mb wind anomalies. (d) Mean May 1996 Reynold SSTA. CI is 0.5°C. Arrows: NCEP WSA. (e) Mean June 1996 NCEP zonal-vertical circulation cross section. The sections are averaged between 1°S-N. The vertical bars represent the eastern and western boundary positions of the American continent. Arrow scales are in the top right corner of each panel.

central and eastern Atlantic (to the west of 10°W), while near the African coast and over the Gulf of Guinea, easterly anomalies appeared at 850 hPa and southern ones at 200 hPa. This resulted in low (upper) troposphere anomalous convergent inflow (divergent outflow) centered near 10°W. This contributed to enhance the convection in this region as evidenced by the negative Outgoing Longwave Radiation Anomalies (OLRA) (Figure 1c), minimum in May–June 1996. These atmospheric anomalies were associated with changes in the Atlantic Walker cell as illustrated on Figure 1e, with anomalous ascending motions over the EA ocean and anomalous descending motions over the neighboring continents. This pattern, opposite to the mean zonal-vertical circulation over the Atlantic, corresponds to the well known weakened and extended eastward Atlantic Walker cell during EA warm conditions [*Wang*, 2002].

4. Long Equatorial Wave Propagations

[9] Based on observations and a forced ocean model, HB00 identify long-equatorial waves during 1995–96. As a first step, we verify their scenario and estimate the skills of the OLM to reproduce the observed anomalies in 1995–96. The OLM is forced with NCEP WSA over 1993–99. Consistently with *Illig and Dewitte* [2006], the model simulates realistic weekly SSTA (SLA) in 1995–96 (Figure 2a), with a correlation/RMS difference between simulation and observations of 0.81/0.29°C (0.68/1.58 cm) in ATL3. This variability is associated with interannual long equatorial wave propagations: The contribution of the Kelvin (K) and first meridional Rossby (R_1) waves to SLA for the most energetic second baroclinic mode [*Illig et al.*, 2004] reveals clear propagations (Figures 2c and 2d) associated with distinct wind events. First, a downwelling Kelvin wave (K1) propagates eastward from December 1995 to February 1996 at approximately 1.3 m/s. It was triggered by strong westerly WSA occurring near South American coast in October–December 1995. This wave reaches the African coast in February 1996, where it reflects as westward propagating Rossby waves. Then, in spring 1996, additional Kelvin wave packets, triggered by intense westerly

WSA in western and central EA, rise the SL, in conjunction with locally-forced downwelling Rossby wave packets (C1), triggered by westward propagating negative WSA in the east (Figure 1a). As pointed out by HB00, this results in overall slow (0.24 m/s) westward-moving SLA with a meridional extension in agreement with a second baroclinic mode first meridional Rossby wave (Figure 2b). This slow propagating signal also imprints the 1996 observed boreal spring-summer SSTA and OLRA (Figures 1b and 1c), which illustrates the importance of local coupled air-sea interactions during the 1996 EA warming.

[10] Thus, in a forced context, the 1996 EA warming seems triggered by an equatorial WSA in Fall 1995, possibly remotely forced by the TP variability (HB00). Then, in spring 1996, the growth of the warming is apparently associated with a westward ocean-atmosphere coupled propagation. Since the EA is a region where air-sea feedback contributes as much to SSTA variability as remote forcing, to further investigate the triggering and the growing
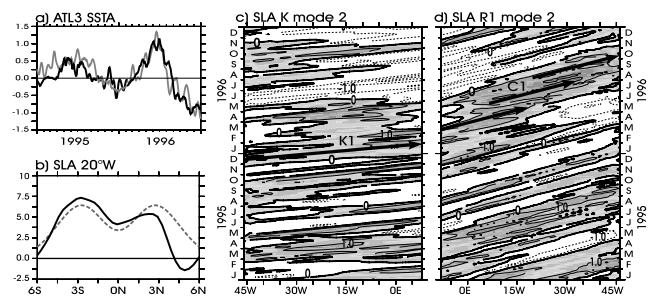

Figure 2. (a) OLM (Reynolds) ATL3 index in black (grey) line. Unit is °C. (b) June 1996 T/P+ERS meridional section at 20°W in plain black. Least mean square fit to the theoretical 2nd baroclinic-mode R_1 mode structure in dashed grey. Unit is cm. (c) Hovmuller of simulated K contribution to SLA for the 2nd baroclinic mode at 0°N. (d) Hovmuller of simulated R_1 contribution to SLA for the 2nd baroclinic mode at 3°N. R_1 is displayed reverse from 46°W to 8°E. CI is 1 cm. Positive values are shaded.

Table 1. Summary of Numerical Experiments Done

Exp.	Name	Forced/Coupled	Prescribed SSTA
1	QTCM-CLIM	Atm. Forced	×
2	QTCM-PAC	Atm. Forced	TP
3	QTCM-CR	Atm. Forced	Globe
4	TIMACS-CLIM	Coupled in EA	×
5	TIMACS-ATL	Coupled in EA	Atlantic, except EA
6	TIMACS-PAC	Coupled in EA	TP
7	TIMACS-CR	Coupled in EA	Globe, except EA

of the 1996 EA event, coupled experiments are carried out with TIMACS over the 1995–96 period.

5. Coupled Experiments

[11] A total of seven model setups (Table 1) are required to interpret the respective part played by the EA local coupled variability and the remote sources of variability in the realization of the 1996 EA warm event. Experiments 1–3 are atmospheric forced simulations, i.e., with no explicit air-sea interactions in the EA, whereas experiments 4–7 consider a full coupling in the EA. The experiments differ by the area of prescribed interannual SST (outside monthly seasonal SST are prescribed as boundary condition for QTCM). For all the experiments, initial conditions are those from TIMACS-CR (Table 1) taken at the 1-Jan-1995. Considering the potential sensitivity of the results to the atmospheric model internal variability, for each experiment setup (forced and coupled), 61 ensemble member simulations are carried out. Each ensemble member is generated by slightly perturbing the TP SST, so that associated atmospheric disturbances can impact the EA variability through the model atmospheric bridges. Perturbations are obtained from observed SST following *Kirtman and Schopf* [1998], namely from the difference between the total and the 6-month low-pass filtered SSTA. Note that TIMACS atmospheric interannual anomalies are estimated with respect to the ensemble mean of the 61 QTCM-CLIM members.

[12] TIMACS-CLIM does not simulate any EA warming over 1995–96 (Figure 3a): the ensemble mean ATL3 index remains close to zero, suggesting no preconditioning of TIMACS to reproduce the 1996 EA warming. Similar results are obtained with TIMACS-ATL (not shown). TIMACS-PAC simulates realistic SSTA peaking in May–June 1996 (Figure 3b), in agreement with the observations (Figure 2a), with somewhat less amplitude. Similar results are obtained with TIMACS-CR (not shown). This demonstrates that the TP conditions in 1995–96 are essential for the generation of the EA 1996 warming in TIMACS. Concurrently, the OLM forced by WSA from QTCM-PAC experiment does not allow for reproducing the magnitude of the observed EA 1996 warm event (not shown), which confirms that local air-sea interactions within the EA participate to the growth of the warm event.

[13] As the results of the coupled experiments point out to the privileged role of the TP in initiating the anomalous 1996 event, we focus on the analysis of the possible teleconnection mechanism between the TP and the EA as observed and simulated by TIMACS.

5.1. Teleconnection Mechanism

[14] From boreal summer 1995 colder than normal conditions are observed in the eastern TP (Figure 1b). The

atmospheric Kelvin wave response causes an anomalous Walker circulation pattern over the equatorial Pacific-Atlantic (Figures 3c–3f). In the far eastern TP, it is associated with a strong air descent, low troposphere divergent outflow and westerly wind anomalies to the east of subsidence area. The model is in good agreement with the NCEP reanalysis, with however different characteristics of the teleconnection pattern depending on the model setup (Figures 3d–3f). Note that a simple vegetation-climate land surface model is embedded in QTCM so that the potential impact of land surface process feedbacks over South America is considered. The strong midtropospheric anomalous descending motion observed over the western part of South America (80°W–75°W) is associated with anomalous divergent low-tropospheric outflow over this region (Figures 3c–3f). Thus, lower-tropospheric westerly wind anomalies develop and reach the western EA in November–December 1995. They induce the WSA (Figure 3a) that force the oceanic Kelvin wave (K1, Figure 2c). Sensitivity experiments with TIMACS indicate that the timing and intensity of these WSA are critical for the 1996 event to develop, as they initiate the warming in the eastern EA (Figures 1a and 2c).

[15] Note also that, in QTCM-PAC, where only TP interannual forcing is considered, the changes in the atmospheric circulation described above and associated WSA in end of 1995 are weaker than in QTCM-CR or in NCEP (Figures 3c–3e), whereas results of TIMACS-PAC compare relatively well to QTCM-CR (Figures 3e–3f). Consistently with *Su et al.* [2005], this illustrates for the Pacific-Atlantic atmospheric bridge, the role of remote local air-sea interactions on teleconnection pattern characteristics.

5.2. Waves Sequence and Air-Sea Feedbacks in the EA

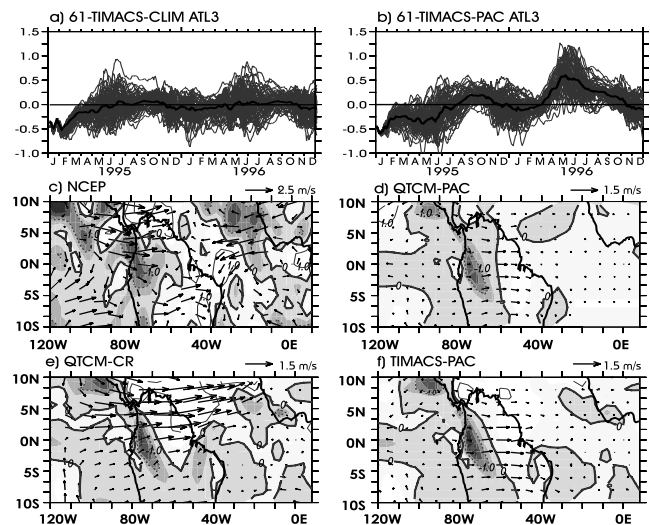[16] We now focus on the growth of the event. The forced downwelling oceanic Kelvin wave (K1) deepens (rises) the

Figure 3. (a) SSTA ATL3 indices for the 61 TIMACS-CLIM ensemble members. (b) SSTA ATL3 indices for the 61 TIMACS-PAC ensemble members. Unit is °C. The thick line is the ensemble mean. (c)–(f) October 1995 anomalous mid-tropospheric vertical velocity (400-600 mb). CI is 1hpa/s. Arrows: 850 mb wind anomalies. Arrow scales are in the top right corner of each panel.

thermocline (SL) along its propagation, increasing the oceanic heat content in Feb–March 1996 in the east EA. The results of OLM suggest that this warming is concurrent with the appearance in February 1996 of downwelling Rossby waves associated with the reflection of K1 (Figures 2c–2d). Moreover, the positive ocean-atmosphere interactions, associated with anomalous convergent inflow in the eastern EA (Figures 4a and 4c), contribute to reinforce and spread the westerly WSA over the whole EA. The latter forces the downwelling Kelvin wave packets in early spring 1996 (Figure 2c) that enhance the warming in the eastern EA. The positive SSTA, together with the low troposphere convergence, result in enhanced convection over the eastern EA in spring–summer 1996 (Figure 4 (left)), which as expected is not simulated in QTCM-PAC. Sensitivity experiments indicate that the negative SSTA in the far eastern TP that is a minimum in April 1996 (Figure 1b) and the associated enhancement of anomalous air subsidence and low troposphere divergence over this region also participate to the westerly WSA intensification over the EA (Figure 4 (right)).

[17] Interestingly, it is at this season that the phase-locking between the interannual variability and the seasonal cycle takes place in the EA [*Latif and Grötzner*, 2000]. This phase-locking is realistically reproduced by TIMACS [*Illig and Dewitte*, 2006]: note the strongest deviations around the ensemble mean in Figures 3a–3b that take place in boreal spring–summer. Therefore, the Kelvin waves triggered in spring 1996 in the far western EA by both convergent inflow in the eastern EA and divergent inflow over South America contribute to the development of warm SST anomalies in EA at the peak phase of the seasonal phase-locking, i.e., when the seasonal weakening of the trade wind in the west and the equatorial upwelling in the east are maximum. We propose that this conjuncture explains the 1996 EA warming.

[18] At the mature phase of the event (June 1996), the equatorial zonal circulation shows a zone of anomalous ascent that extends eastward and takes place over almost the whole EA up to Greenwich line, with descending motion confined in the Gulf of Guinea and on the western Africa (Figures 1e and 4). In the low troposphere, the convergent flow is associated with easterly anomalous winds in the far eastern EA which contribute to the convergence and the enhanced convection over the warm SSTA region (Figures 1c and 4). The westward displacement of the warm SSTA and the cooling in the far eastern EA (Figure 4 (left)) are associated with coupled instabilities that advect the SSTA through non linear processes. The latter are associated with downwelling Rossby waves from the reflection of the Kelvin waves and intensified by the anomalous easterlies in the far eastern EA (Figures 1a and 2d).

6. Summary and Conclusions

[19] The 1996 warming in the EA is documented and interpreted through the comparison of observations and ensemble simulations of an intermediate coupled model of the Tropical Atlantic. It is shown that a simple linear model is able to simulate most aspects of this particular warming (phase and amplitude), with skills comparable to OGCMs [*Illig and Dewitte*, 2006]. This points out to the privileged role of the equatorial wave dynamics and confirms HB00's
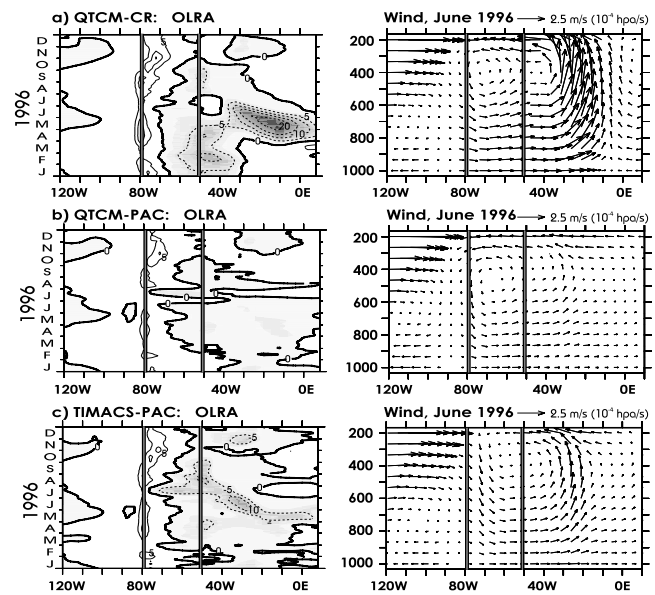

Figure 4. (left) Hovmuller of OLRA. CI is 5 W/m^2. (right) Mean June 1996 zonal-vertical circulation cross section (scale in the top right corner). The sections are averaged between 1°S-N. The vertical bars represent the eastern and western boundary positions of the American continent.

results. Consistently with their study, the analysis of the ocean-atmosphere feedbacks associated with the changes in the Atlantic Walker circulation suggests that the 1996 warming is the signature of the Atlantic equatorial coupled mode [*Zebiak*, 1993], triggered by WSA in November–December 1995. Atmospheric teleconnections are further documented in the model and in the NCEP reanalysis. Results indicate that anomalous air descent and low-tropospheric divergence over South America associated with cold conditions in the eastern TP led to the WSA in end of 1995 that forced downwelling Kelvin waves in the EA. Persistent anomalous conditions in the eastern TP further enhanced the anomalous westerlies over the EA in boreal spring 1996 when the seasonal phase-locking is expected.

[20] Although with a tendency to underestimate the 1996 EA warming, our coupled model does simulate a rectification of the EA variability by the TP oceanic conditions and the results of various experiments with this model support the proposed scenario of teleconnection. Interestingly, in June 1999, warm SSTA (~1°C) were observed in EA, while anomalous cold conditions in the TP were observed from Avril 1998 until mid-2000. Whether or not similar teleconnection mechanisms were at play at that period would deserve further investigation in order to test if our result could have prediction application/implication.

References

Delecluse, P., J. Servain, C. Levy, K. Arpe, and L. Bengtsson (1994), On the connection between the 1984 Atlantic warm event and the 1982–83 ENSO, *Tellus, Ser. A, 46*, 448–464.

Handoh, I. C., and G. R. Bigg (2000), A self-sustaining climate mode in the tropical Atlantic, 1995–97: Observations and modelling, *Q. J. R. Meteorol. Soc.*, *126*, 807–821.

Illig, S., and B. Dewitte (2006), Role of local coupled equatorial variability versus remote ENSO forcing in an intermediate coupled model of the tropical Atlantic, *J. Clim.*, in press.

Illig, S., B. Dewitte, N. Ayoub, Y. du Penhoat, G. Reverdin, P. De Mey, F. Bonjean, and GSE Lagerloef (2004), Interannual long equatorial waves in the tropical Atlantic from a high resolution OGCM experiment in 1981–2000, *J. Geophys. Res.*, *109*, C02022, doi:10.1029/2003JC001771.

Kalnay, E., et al. (1996), The NCEP/NCAR 40-year reanalysis project, *Bull. Am. Meteorol. Soc.*, *77*, 437–471.

Kirtman, B. P., and P. S. Schopf (1998), Decadal variability in ENSO predictability an prediction, *J. Clim.*, *11*, 2804–2822.

Latif, M., and A. Grötzner (2000), The equatorial Atlantic oscillation and its response to ENSO, *Clim. Dyn.*, *16*, 213–218.

Le Traon, P. Y., F. Nadal, and N. Ducet (1998), An improved mapping method of multisatellite altimeter data, *J. Atmos. Oceanic Technol.*, *15*, 522–534.

Neelin, J. D., and N. Zeng (2000), A quasi-equilibrium tropical circulation model-formulation, *J. Atmos. Sci.*, *57*, 1741–1766.

Reynolds, R. W., and T. M. Smith (1994), Improved global sea surface temperature analyses using optimum interpolation, *J. Clim.*, *7*, 929–948.

Su, H., J. D. Neelin, and J. E. Meyerson (2005), Mechanisms for lagged atmospheric response to ENSO SST forcing, *J. Clim.*, *18*, 4195–4215.

Wang, C. (2002), Atlantic climate variability and its associated atmospheric circulation cells, *J. Clim.*, *15*, 1516–1536.

Zebiak, S. E. (1993), Air-sea interaction in the equatorial Atlantic region, *J. Clim.*, *6*, 1567–1586.

————————————
N. Ayoub, B. Dewitte, Y. du Penhoat, and S. Illig, LEGOS, 14 avenue Edouard Belin, F-31401 Toulouse, France. (illig@notes.cst.cnes.fr)

D. Gushchina, Geographical Faculty, Moscow State University, Moscow 119899, Russia.